ACS Symposium Series, vol. 804
Oxford University Press, 2002
"Polymer Nanocomposites"
eds. R. Vaia & R. Krishnamoorti

Chapter 15

Molecular Simulations of Ultra-Confined Polymers. Polystyrene Intercalated in Layered-Silicates.

E. Manias [1], V. Kuppa

Materials Science & Engineering department,
The Pennsylvania State University, University Park, PA

Abstract

Molecular Dynamics simulations are used to explore the structure and dynamics of polystyrene confined in $2nm$ slit pores, between surfactant-bearing mica-type surfaces. The systems simulated resemble experimentally studied intercalated nanocomposites, where polystyrene is inserted between alkyl-ammonium modified fluorohectorite silicate layers. The molecular modeling perspective complements the experimental findings and provides insight into the nature of polymers in nanoscopic confinements, especially into the molecular origins of their macroscopic behavior. Namely, simulations show a distribution of relaxations, ranging from extremely faster and to much slower segmental motions than the ones found in the corresponding bulk polymer at the same temperature. The origins of these dynamical inhomogeneities are traced to the confinement induced density modulations inside the 2nm slits. Fast relaxing phenyl and backbone moieties are found in low density regions across the film, and preferentially in the center, whereas slow relaxing moieties are concentrated in the denser regions, especially in the immediate vicinity of the confining surfaces.

Introduction

Polymers in nanoscopic confinements possess remarkable dynamical heterogeneities which vary on length scales as short as a few Angstroms [1,2], and manifest themselves macroscopically in a variety of unusual properties. Model systems, that can be interrogated experimentally to study ultra-thin [$\sim$2-5nm] polymer films confined between solid surfaces, can be created by intercalating high molecular weight polymers in between alluminophyllosilicates [mica-type layered crystals]. Especially where appropriately modified silicates are used to form intercalated nanocomposites, very homogeneous ultra-thin confined polymer structures self-assemble in multilayer

[1] address correspondence to: manias@psu.edu

systems, that can be designed to consist exclusively of identical nanoconfined films, and no free –unconfined– polymer [3, 4]. These intercalated materials offer great potential for the study of polymers and liquids in extreme confinements [1-2nm] by employing conventional analytical techniques [3–6].

For this reason, intercalated polymer/silicate nanocomposites have been recently investigated with the emphasis on the fundamentals of nanoscopically confined polymers [5, 6]. It has been found that the nanoscopic confinement between solid surfaces affects the polymer behavior in ways that are not intuitively expected. Additionally, in many cases this confinement-modified polymeric structure and dynamics have been shown to dictate the materials response at the macroscopic level [3], causing remarkable enhancements of the materials properties [4].

Here, we report a molecular modeling approach, motivated by the previous experimental studies, aiming in obtaining insight into the confinement induced dynamical processes of ultra-thin polystyrene films in 2nm slit pores. Studying the formation, structure and dynamics of these intercalated structures can lead to a better understanding of polymers in a confined environment or at a solid interface, and at the same time provide the necessary fundamental level knowledge towards the molecular design of polymer/inorganic hybrid materials with desirable properties.

Simulation Model and Details

Inspired by striking new experimental findings of polymer films in 2nm slit pores between alkyl-ammonium modified mica-type surfaces [5, 6], we performed extensive Molecular Dynamics (MD) computer simulations of polystyrene (PS) in 2nm slits. Since details about the simulation method and model are given in length elsewhere [7], here we will only mention some of the essential information.

Simulation geometry. The simulation geometry resembles closely the systems studied by NMR [6]. Our simulation box is 2.112×1.828×3.05 nm in dimensions, with periodic boundary conditions in all three directions [figure 1]. A solid surface with the crystal structure of a synthetic 2:1 mica-type silicate is placed parallel to the xy plane, thus confining the organic molecules in the z direction. The confinement size [3.05nm] was selected to correspond to the experimentally measured X-ray diffraction d-spacing [3] and, after subtracting the wall thickness, it allows for a 2.05nm thin film of organics between the two solid surfaces. The MD runs were carried out in an NVT ensemble, where the number of particles (N) is chosen based on the experimentally measured material amounts. The grafting density of the surfactant chains [which are octadecyl-ammonium molecules] is well-known and characteristic of the silicate surface [8]. Our grafting density [σ_{graft}=$1/0.97nm^2$ on each wall] corresponds to fluorohec-

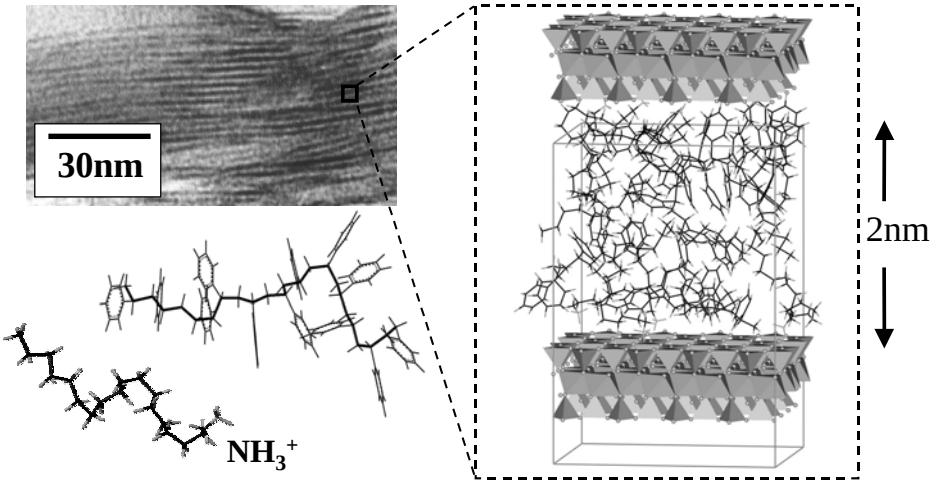

Figure 1 *The system under investigation. From top left clockwise: a bright-field TEM detail of the PS/octadecyl-ammonium silicate intercalate [6]; a snapshot of the simulation box; a styrene 12mer (the smaller of the two PS molecules simulated) and the octadecyl-ammonium surfactant molecule.*

torite [8], which is the silicate used in the NMR studies, and dictates 8 octadecyl-ammonium cations over the two solid surfaces. Furthermore, from thermogravimetric analysis (TGA) the polymer to surfactant weight ratio can be measured [3], and necessitates for 36 styrene monomers in the slit. Two systems were extensively studied, the first with 3 styrene chains of 12 monomers each, and the second with 3 chains of 24 monomers [in this case the box size is 2.112×3.656×3.05nm with 16 surfactant molecules]. Although these chains may be too short to capture the genuine response of long PS macromolecules, they are both longer than the average physisorbed train size of PS in these systems, and also allow for the existence of bridges between the two solid surfaces. Consequently, all the possible segmental dynamics that can develop inside these slit pores can be explored by our MD. Moreover, comparing the two systems with different PS chain lengths does not show any differences *in the segmental dynamics* discussed herein, albeit the substantially longer *chain relaxation times* of the confined 24mer compared to the 12mer.

Force-field. The force-fields for polystyrene, and its interactions with the alkyl-ammoniums [tabulated in table 1], are the same as recent PS simulations by Müller-Plathe [9]. The interactions between the silicate and the organic molecules [styrene and aliphatic chains] is based on our previous simulation work on organic/silicate complexes [8, 10].

Table I. The force-field used in the simulations.

Bonded and non-bonded interactions for the organic species are given [7, 9].

non-bonded	$V(r_{ij})=4\epsilon\,[(\sigma/r_{ij})^{12}-(\sigma/r_{ij})^{6}]+(1/4\pi\epsilon)\,q_i\,q_j/r_{ij}$		
interactions	σ [nm]	ϵ [KJ/mol]	q [e]
C	0.3207	0.3519	0.000
C_{ph}	0.3550	0.2940	0.115
C^{a}_{ph}	0.3550	0.2940	0.000
H	0.2318	0.3182	0.000
H_{ph}	0.2420	0.1260	-0.115
N	0.2976	0.8767	1.000
bond-stretching	$V(r)=(k_b/2)\,(r-b_o)^2$		
potentials	b_o [nm]	k_b [KJ/mol]	
C - C	0.153	334720	
C_{ph} - C	0.151	418400	
C_{ph} - C_{ph}	0.139	418400	
C - N	0.133	376560	
C - H	0.109	292880	
C_{ph} - H	0.108	292880	
N - H	0.100	374468	
bond-angle	$V(\theta)=(k_\theta/2)\,(\theta_{ijk}-\theta_o)^2$		
potentials	θ_o [deg]	k_θ [KJ/(mol rad^2)]	
H - C - H	109.45	306.40	
C - C - H	109.45	366.90	
C_{ph} - C - H	109.45	366.90	
C - C - C	109.45	482.30	
C - C - C_{ph}	109.45	482.30	
C - C_{ph} - C_{ph}	120.00	376.60	
C_{ph} - C_{ph} - C_{ph}	120.00	376.60	
C_{ph} - C_{ph} - H	120.00	418.80	
H - N - H	109.45	306.40	
N - C - H	109.45	366.90	
C - C - N	109.45	482.30	
proper	$V_{ijkl}(\phi)=k_\phi\,[1+\cos(n\phi-\phi_o)]$ $\phi_{cis}=0^\circ$ & $\phi\equiv(ijk)\angle(jkl)$		
dihedrals	ϕ_o [deg]	k_ϕ [KJ/mol]	n
C - C - C - C	0.0	5.88	3
C - C - C - N	0.0	5.88	3
C - C - C - H[b]	0.0	5.88	3
C - C - N - H[b]	0.0	5.88	3
planar (improper)	$V_{ijkl}(\xi)=k_\xi\,(\xi-\xi_o)^2$, i central C_{ph} and $\xi\equiv(ijk)\angle(jkl)$		
dihedrals		ξ [deg]	k_ξ [KJ/mol]
C_{ph} - C_{ph} - C_{ph} - C_{ph}		0.0	167.36
C^{i}_{ph} - C_{ph} - C_{ph} - H_{ph} [on i]		0.0	167.36
C^{i}_{ph} - C_{ph} - C_{ph} - C [on i]		0.0	167.36

[a] the phenyl carbon connected to the backbone methine.

[b] the hydrogens of the chain-end methyls and ammoniums.

The solid surface atoms were constrained to their equilibrium positions via harmonic springs, which allowed for thermal vibration; comparative studies with completely immobilized solid atoms did not reveal any differences in the results discussed herein. The temperature was stabilized via a weak coupling to a heat bath by the Berendsen thermostat [11]. Since the silicate surface is negatively charged [for fluorohectorite -$1q_e/0.97nm^2$] the positive ammoniums have a strong Coulombic attraction to the surfaces, effectively end-tethering the octadecyl-ammoniums on the surfaces.

Initial configurations, and ensemble. Probably the most crucial and important aspect of these simulations is the way we selected to sample the configuration phase-space. A simple Configurational Biased Monte Carlo (CBMC) scheme was developed to produce alkane surfactant configurations [12]. For the polystyrene molecules however –where the phenyl sidechains prohibit the use of a simple CBMC approach– a more elaborate route was necessary: The rotational-isomeric-state (RIS) model was used to create initial polymer conformations of PS. Conformations that fit in the interlayer gallery were chosen, and equilibrated by an off-lattice Monte Carlo scheme that employs small random displacements of the backbone atoms and Orientational Biased Monte Carlo rotations of the phenyl rings; the surfactants were equilibrated by CBMC attempts in coexistence with the polymer chains [12]. It is *critical* to have many independent, well-equilibrated initial configurations of the systems to be simulated: As the polymer is held together by strong covalent bonds, the relaxation of the chains is determined by the *slowest* moving segments along the polymer. Even though mobile segments are expected to exist in large numbers [6] they will be bonded to portions of the polymer that remain "frozen" for timescales vastly longer than what is accessible through MD. Therefore, the only realistic way to explore a large portion of the configurational space is to start with many *independent* initial system conformations and perform productive MD simulations of a few (10-100) nanoseconds. Typically, we used 10 independent initial configurations for each temperature and we followed each system for 100ns at T=350K, 50ns at T=370 and 390K, and 10ns at higher temperatures.

Polystyrene in 2nm thin slit pores

Structure of the confined film. In figure 2 the partial density profiles across the slit pore are shown for different components of the confined organic film. These density profiles correspond to the probability of finding the corresponding groups at a certain distance away from the confining solid surfaces, and are calculated through NVT ensemble averages of productive MD runs starting from *distinctly different* initial system configurations. The usage of several –typically ten– different initial configurations for each simulated temperature is essential, because the relaxation times of both

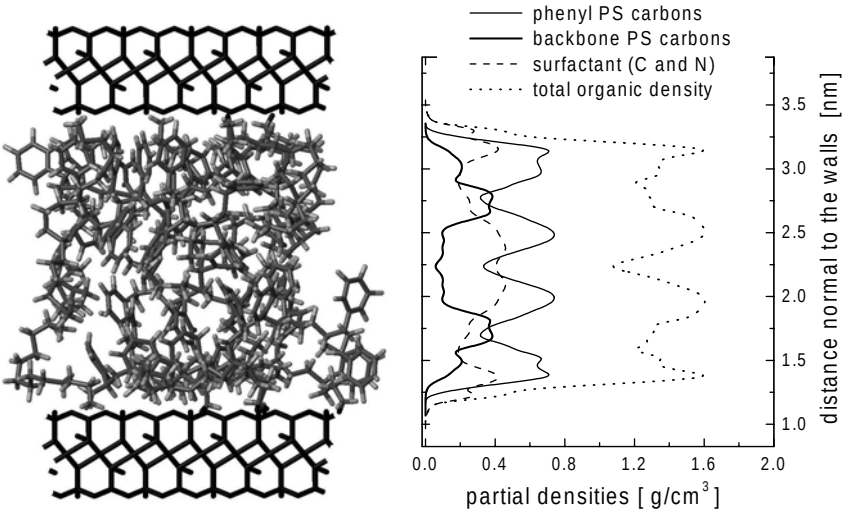

Figure 2 *Density profiles across the interlayer gallery. Partial densities of the surfactant carbons and nitrogens (dashed line), the styrene phenyl carbons (light continuous line), styrene methyl, methylene and methine carbons (heavy continuous line), and the total organic density (dotted line) across the slit pore are shown.*

the surfactant molecules and styrene chains reach far beyond the 10-100ns time periods simulated in each MD run. The same density profiles can also be calculated based solely on the Monte Carlo scheme used to create the initial systems for the MD, and are the same with the MD profiles within the data accuracy. This agreement between the MC and the MD ensembles is an indication that our MD's actually sample a representative portion of the phase-space.

From figure 2 is obvious that the mass is distributed across the slit pore in a highly inhomogeneous layered fashion. This kind of layering is seen in all simulations of confined systems [ranging from small molecule simple liquids, to alkane oligomers, to grafted alkanes, to generic Lennard Jones chains and realistic polymers]. This layering normal to confining surfaces is attributed to the steric interactions between the walls and the confined fluids, and is macroscopically manifested in SFA experiments by wildly oscillating solvation forces, when confined fluids are squeezed between mica surfaces [13].

In this system, however, there exist several species across the gallery [such as ammonium and aliphatic surfactant groups, as well as aliphatic and aromatic styrene groups] and a preferential layering with respect to the walls is developed. The positively charged ammoniums are found in

direct contact with the silicate walls –even at the highest temperatures studied– whereas most of the aliphatic part of the surfactant is preferentially located at the center of the slit [figure 2]. At the same time, we find that the polymer backbone is predominately located in two well-defined layers, at distances of about 0.3-0.7 nm from each solid surface. Often, a short strand of polymer adopts a bridging configuration perpendicular to, and connecting between, both walls. The phenyl rings, which attach to the backbone at each methine, are similarly found on either side of the backbone, and dominate the organic matter nearest the silicate surface. Finally, while surfactant methylenes are found distributed all across the slit pore, they bunch preferentially in the middle layer. These trends provide some clues as to the origin of the confined film structure: The polar phenyl groups, that interact strongly with the silicate surface, are preferentially located closest to the surface, whereas the aliphatic groups are displaced towards the center of the pore. Obviously, due to the covalent bonds between the styrene phenyls and methines, the backbone cannot be displaced completely in the center of the pore. Similarly, as the head group of the surfactant is tethered via an ionic interaction to the negatively charged silicate, the surfactant cannot be completely displaced from the surface either. As a result, only its aliphatic tails are displaced by the PS in the center of the slit [figure 2].

At first glance, all this detail may seem too theoretical. However, the surface sensitive ^{1}H-^{29}Si cross-polarization NMR does provide a direct check of the validity of this layered structure (fig. 4 in [6]). This NMR approach does support the above structural description, and finds the styrene segments –phenyls and backbones– close to the surfaces and the surfactant tails removed towards the center of the slit [6]. Moreover, NMR spectroscopy provides insight on the segmental dynamics of the various moieties in the slit pore, as discussed in the next paragraph.

Segmental dynamics of PS in 2nm slit pores. A combination of surface sensitive ^{1}H-^{29}Si cross-polarization NMR and quadrupolar echo ^{2}H NMR was used to study the segmental dynamics of selectively deuterated PS in 2nm slit pores [6]. From these recent NMR studies a new and quite unexpected picture is emerging for the dynamics of nanoscopically confined polymers, which was further confirmed by dielectric spectroscopy investigations on a polysiloxane system [5]. Namely, a coexistence of fast and slow segmental dynamics is observed over a wide range of temperatures, below and above the bulk T_g. This very wide distribution of segmental dynamics spanned relaxation times that ranged from much faster to much slower than the ones observed in the bulk for all temperatures studied: Very fast motions were observed in the confined polymer for temperatures deep below the bulk T_g, where the corresponding bulk polymer was essentially in a solid-like, immobilized, glassy state [6]; while for temperatures above the bulk T_g, there still exist many segments that remain solid-like and im-

mobilized in the confined systems [6], when at the same temperatures the bulk PS is in a molten, liquid-like state.

Our computer modeling approach aims to unveil the molecular origins of these dynamical inhomogeneities. To this end, we simulated the system depicted in figure 1 for several temperatures in the same T-range of the ^{2}H NMR experiments. We monitor segmental mobility much like the NMR is doing, by following the relaxation of the C-H bond reorientation. Beyond translation, one can define two types of phenyl reorientations: the "flipping" around the phenyl axis, and the "rocking" of this axis. For the backbone methylenes and methines, C-H reorientation takes place by trans-to-gauche isomerization. For NMR, "mobile" are those C-H bonds that are characterized by relaxation times smaller than the NMR echo spacing [τ=20μs]. In our simulations, and focusing on the phenyl dynamics, we define as mobile those phenyls that are characterized by relaxation times shorter than τ, as measured from the time autocorrelation function of the corresponding C-H bond vectors, or equivalently by the phenyl "flip axis" $\vec{u}(t)$ and/or the normal vector that defines the "rocking axis" [figure 3].

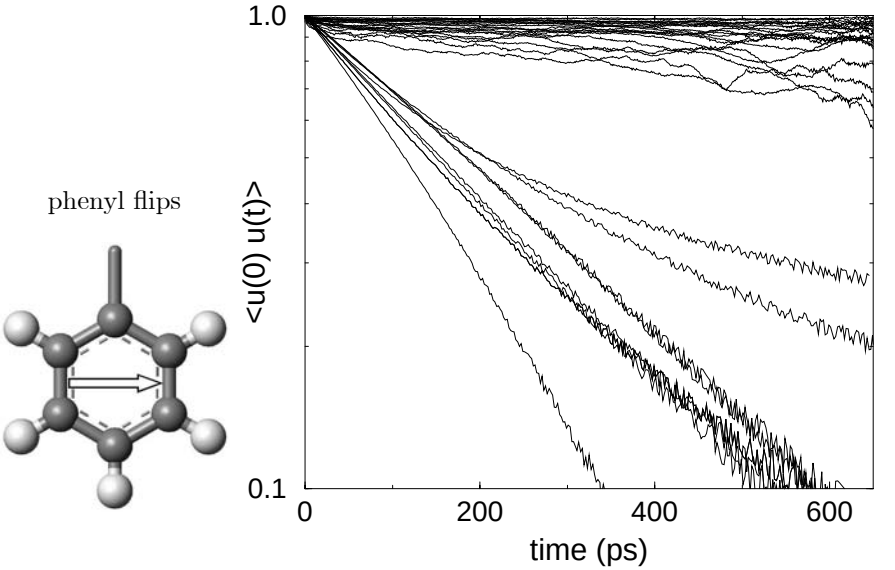

Figure 3 *Time autocorrelation function of the phenyl flip vector [$\vec{u}(t)$, shown on the left], for the intercalated PS phenyls at 420K. An ensemble average is calculated over all runs starting from different initial configurations and over multiple time origins in each trajectory of 10ns.*

A few of the $\langle \vec{u}(0) \cdot \vec{u}(t) \rangle$ in figure 3 correspond to ultra-fast flipping phenyls, with typical rotational relaxation times (τ_R) of a few tens/hundreds of *ps*. These are characteristic of PS and are also observed in bulk PS [9], albeit in much smaller populations. The confinement-induced dynamical in-

homogeneities are seen in the family of curves with longer τ_R [smaller slopes correspond to longer relaxation times]. In figure 3 there is a distibution of flip-relaxation times that characterizes the majority of the system's phenyls, and spans the range from 20ns to "infinity" [i.e. lines with slope zero, that correspond to phenyl rings that are immobilized throughout the duration of the MD run]. This distribution of τ_R is typical for all temperatures simulated [350-420K] as far as the relaxation times are concerned, although the number of phenyl rings with faster τ_R is an increasing function of temperature. The other modes studied [7] [phenyl rocking, backbone trans-gauce isomerization] have similar behaviour as the one seen for the phenyl flipping. This distribution of relaxation times is actually confinement-induced, and evidence to this end is provided in the next paragraph.

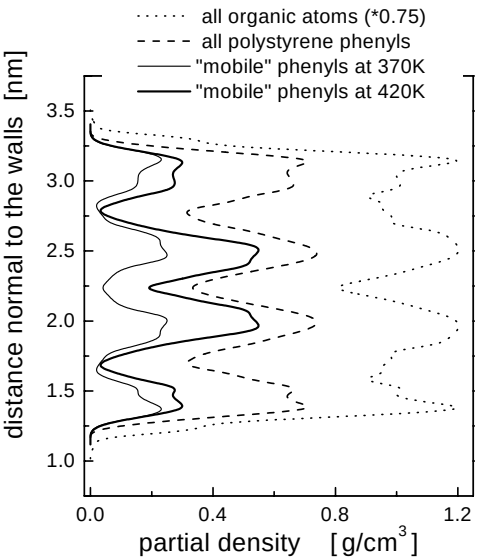

Figure 4 *Density profiles normal to the silicates: for all the phenyl carbons (dashed line) and those carbons belonging to mobile phenyls (at 370K light line, and 420K heavy line). With ascending temperature the number of mobile phenyls increases, as can be enumerated by the area under the corresponding profiles, and at the same time, the mobile phenyls are preferentially located in the center of the slit.*

Origin of the dynamical heterogeneities. Still focusing on the phenyl ring dynamics, we show in figure 4 the distribution of the carbons belonging to "mobile" phenyl rings, for two temperatures [370K and 420K]. In figure 5a we quantify the percentage of mobile phenyls as a function of temperature. With increasing temperature the number of mobile phenyls increases, and also these mobile rings are located increasingly in the center

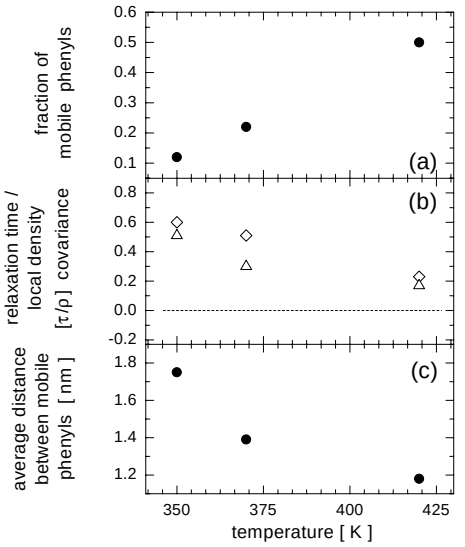

Figure 5 (a) *the mobile fraction of phenyls: corresponding to fast orientational relaxations through ring "flips" and/or axis "rocking".* (b) *the covariance of the relaxation time and the local density for the mobile phenyls* [◇ *flipping,* △ *rocking*]. (c) *the average distance between mobile phenyls: the decrease with T is due to the increased number of mobile phenyls, and also their tendency to preferential concentrate in the middle of the slit pore bunched in groups.*

of the pore; this trend is in agreement with the NMR observations. Since the mobile phenyls are located both in the center of the slit pore, as well as near the surfaces –albeit in smaller numbers– the fast segmental dynamics do not seem to originate from the location of the segments across the pore, as in wider confined alkane films [14]. Motivated from MD simulations in glass forming simple liquids [15], we can check the correlation between the segmental dynamics and the *local* structure inside the confined film. This can be realized through the estimation of the covariance of the segmental relaxation and the local density, defined as:

$$\mathrm{cov}(\tau,\rho) \equiv \frac{\langle\ (\tau - \langle\tau\rangle)\cdot(\rho - \langle\rho\rangle)\ \rangle}{\sqrt{\sigma^2(\tau)\ \sigma^2(\rho)}} \tag{1}$$

where, τ is the segmental relaxation time of a particular phenyl, $\langle\tau\rangle$ is the ensemble average over all phenyls, $\langle\rho\rangle$ is the average density across the slit pore, and ρ is the local density around the phenyl in question. $\sigma^2(\tau)$ and $\sigma^2(\rho)$ are the ensemble variances of the relaxation times and density

respectively. Following this definition, maximum correlation between fast segmental relaxations and low local densities [or equivalently slow segmental relaxations and high local densities] yields a value of $\mathrm{cov}(\tau,\rho)=+1$. Or, for the mobile phenyls of figure 5a:

$$\mathrm{cov} = \begin{cases} +1 & \text{fast segmental dynamics at local density minima} \\ 0 & \text{no correlation between dynamics and density} \\ -1 & \text{fast segmental dynamics at local density maxima} \end{cases}$$

The relaxation time/local structure covariance for the mobile phenyls is shown in figure 5b. For the lower temperatures simulated there exists a strong correlation between the local structure and the segmental relaxation. Namely, the fast relaxing phenyls are located in regions where the local density is low [independent of whether they are close to the walls, or in the center of the slit; and independent of whether the C-H relaxation takes place through "flipping" or "rocking" motions]. As the temperature increases this correlation seems to decay in magnitude, although it still remains positive.

In fact, as the temperature increases, the number of mobile phenyls also increases in such a degree that large volumes in the middle part of the slit consists solely of phenyls with fast segmental dynamics. This reflects in a decreasing average distance between fast relaxing phenyls [as seen in figure 5c]. Furthermore, careful analysis of the MD trajectories reveals that at the lower temperatures there exist a few only segments with fast dynamics, which are isolated from each-other inside the confined film. As the temperature increases, "clusters" of mobile phenyls are formed, especially in the center of the slit pore [figure 6]; however, despite their proximity, the motions of the phenyls within the same "cluster" are not correlated nor cooperative. For all the temperatures simulated [even above 420K] there exists a large number of immobilized phenyl rings in the immediate vicinity of the confining surfaces, where the organic film is locally densified by the silicate surfaces. The relaxation of these slow phenyls is markedly temperature independent, at least for the time scales that our MD simulations probe. This is in general agreement with the cross-polarization NMR studies, which suggest that styrene moieties in the center of the slits are more mobile, while chain elements [phenyls, methylenes, and methines] interacting with the surface are dynamically inhibited.

Similar analysis for the backbone segmental dynamics reveals the same trends as discussed above for the phenyls [7]. That is, fast backbone segmental dynamics are predominately found in regions where the local density is low, and with increasing temperature mostly in the center of the slit pore. Furthermore, an interesting observation is that the fastest relaxing phenyls are covalently bonded to the fastest backbone segments, and the same for the slowest moving backbones and phenyls. This was not obvious, or intuitively expected, as the phenyl segmental relaxation [e.g. through flipping] does not require backbone reorientation. For example, in bulk –unconfined– PS chains phenyl modes are enabled at temperatures below T_g where the

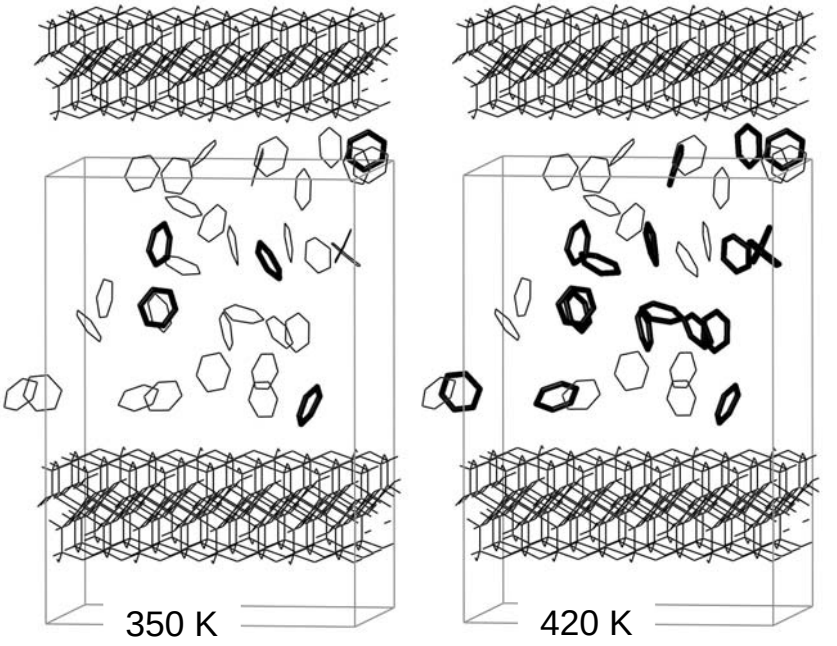

Figure 6 *All the PS phenyls are shown and the ones with fast segmental dynamics are highlighted [hydrogen atoms, polymer backbones, and surfactant molecules are omitted for clarity]. To promote comparison, the same system configuration at two different temperatures is shown. At 350K the mobile phenyls are isolated in parts of the system where the local density is low. At 420K regions of closely bunched phenyls with fast segmental dynamics develop, especially in the center of the slit, but there also still exist isolated mobile phenyls in the low local density regions also near the confining walls.*

backbone remains rigid; backbone modes start only near T_g. Although a more detailed analysis is necessary, this connectivity between moieties with fast segmental relaxations could be the reason that the phenyl and the backbone dynamics are strongly coupled in the confined films [6].

Effect of the surfactant. Due to the existence of a large number of alkyl-ammonium molecules in our confined systems, that can "plasticize" the polymer, it was not initially clear [6] whether these dynamical inhomogeneities arise from plasticization effects, or whether are confinement induced. On this point, our simulations show that the fast segmental relaxations are not correlated to the surfactant proximity and/or dynamics [figure 7], but originate from the confinement-induced density inhomogeneities [figure 5].

This is further supported by other experimental studies of different sys-

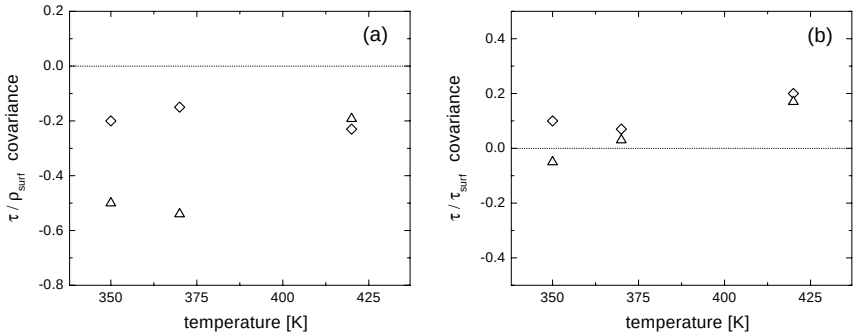

Figure 7 (a) *The covariance between the fast phenyl dynamics and the local surfactant density (ρ_{surf})* [◇ *flipping,* △ *rocking*]. *The existence of surfactant monomers next to the phenyls seems to inhibit fast phenyl dynamics [especially fast "rocking" relaxations]. This is not surprising as the alkyl surfactants can pack much more effectively around the phenyls, than the other styrene monomers, and thus increase the local density promoting slower relaxations in their vicinity.* (b) *The covariance between the phenyl relaxation and neighboring-surfactant relaxation. Except for the highest temperature there seems to be no correlations between the phenyl and neighboring-surfactant dynamics, i.e. the fast phenyls are not preferentially located next to fast surfactants, and the slow phenyls are not preferentially located next to slow relaxing surfactants. For the highest temperature, there exists a correlation since all moieties [surfactants and phenyls] near the surfaces are slow relaxing [dynamically inhibited], whereas in the center of the gallery all moieties relax faster.*

tems, which also provide strong indications that these segmental dynamical are associated with the polymer confinement: ***(i)*** ^{2}H NMR lineshape studies by Zax and coworkers, also observed coexisting fast and slow modes in poly(ethylene oxide) which was intercalated in the same silicate as the PS herein, but in absence of any surfactant whatsoever [16]. In this case, despite the much narrower confinements [0.8nm], the intercalated PEO chains exhibit substantial segmental motion [16]. ***(ii)*** dielectric spectroscopy of poly(methyl phenyl siloxanes) [with a T_g more than 150K below the PS T_g] report a similar coexistence of ultra-fast and solid-like (slow) relaxations over a wide range of temperatures [5], and measure an extraordinarily fast relaxation which is completely absent in the bulk -unconfined- polymer.

Comparison to experiments. Finally, we would like to commend on the quantitative comparison between the molecular simulations and the NMR experiments. The simulation enumeration of the mobile fraction underestimates the NMR measured one [6], albeit capturing the correct temperature dependence. This discrepancy can result from several sources,

such as the uncertainties in the relaxation time calculation, and phenomena that become important after the 100ns probed by our MD runs [such as polymer diffusion or desorption]. However, none of these two reasons can adequately account for the deviation between the experimental and simulation values. We believe that the cause of this difference lies in the organic [styrene and alkyl-ammonium] density used in our simulations, which must be higher than the ones in the intercalated experimental systems. Even though we based our densities on the TGA estimated quantities, the gravimetric method may also measure polymers physisorbed on the outside of the silicate stacks, i.e. not in the confined film. Since there exists a very strong dependence between the density and the fast segmental dynamics, minute deviations in density can result in large variations in the system dynamics. Nevertheless, the aim of the simulations is not to quantitatively reproduce the experimental observations, but to reveal the origins of the experimentally observed behavior, and provide insight to the relevant molecular processes. To this end, we feel that the present study was quite successful.

Conclusions

Molecular modeling approaches are employed to explore polystyrene molecules confined in 2nm slit pores, resembling intercalated PS in octadecyl-ammonium modified layered-silicate surfaces. The simulations show that the confined film adopts a layered structure normal to the solid surfaces, with the polar phenyls dominating the organic material adsorbed on the walls, and the aliphatic groups predominately in the center of the pore. This layered structure, with the polar styrene groups preferentially on the surfaces, reflects on previous ^{1}H-^{29}Si cross-polarization NMR measurements.

A distribution from ultra-fast to solid-like slow segmental dynamics exists across a wide temperature range, below and above T_g, for both the styrene phenyl and the backbone groups. The mobile moieties concentrate at the center of the slit pore, especially for the higher temperatures. The MD simulations attribute these dynamical inhomogeneities to confinement-induced density inhomogeneities. Namely, the moieties with fast segmental dynamics are located in local density minima. Moreover, MD show that at low temperatures the fast moving species are isolated throughout the confined film, whereas with increasing temperature the mobile moieties increase in number and bunch up in groups, especially in the middle of the pore.

Acknowledgement This work was supported by a Wilson Research Initiation grant from the EMS College at Penn State. We also acknowledge the GroMaCS group of Groningen Univ. (Netherlands) for helpful discussions.

References

[1] I. Bitsanis and C. Pan. *J. Chem. Phys.*, **1993**, *99*, 5520.
S. Granick, *Science*, **1991**, *253*, 1374.

[2] E. Manias, G. Hadziioannou, and G. ten Brinke. *Langmuir*, **1996**, *12*, 4587; *Europhys.Lett.*, **1993**, *24*, 99; *Europhys.Lett.*, **1996**, *33*, 371.

[3] E.P. Giannelis, R.K. Krishnamoorti, and E. Manias. *Advances in Polymer Science*, **1998**, *138*, 107.

[4] M. Alexandre, P. Dubois. *Mat. Sci. & Eng. R: Reports*, **2000**, *28*, 1.

[5] S.H. Anastasiadis, K. Karatasos, G. Vlachos, E.P. Giannelis, and E. Manias. *Phys. Rev. Lett.*, **2000**, *84*, 915.

[6] D.B. Zax, D.-K. Yang, R.A. Santos, H. Hegemann, E.P. Giannelis, and E. Manias. *J. Chem. Phys.*, **2000**, *112*, 2945.

[7] V. Kuppa and E. Manias. *Colloids & Surfaces A, in press.*, **2001**.

[8] E. Hackett, E. Manias, E.P. Giannelis. *J.Chem.Phys.*, **1998**, *108*, 7410.

[9] F. Müller-Plathe. *Macromolecules*, **1996**, *29*, 4782.
(updated information on the PS force-field can be found at Müller-Plathe's web site at the Max-Planck Instistute, Mainz, Germany).

[10] E. Hackett, E. Manias, E.P. Giannelis. *Chem. Mat.*, **2000**, *12*, 2161.

[11] H. J. C. Berendsen, J. P. M. Postma, W. F. van Gunsteren, A. Di Nola, and J. R. Haak. *J. Chem. Phys.*, **1984**, *81*, 3684.

[12] E. Hackett, E. P. Giannelis, and E. Manias. *J. Chem. Phys., in press.*

[13] H. K. Christenson. *J. Chem. Phys.*, **1983**, *78*, 6906; D.Y.C. Chan and R.G. Horn, *J. Chem. Phys.* **1985**, *83*, 5311; J.P. Montfort and G. Hadziioannou, *J. Chem. Phys.* **1988**, *88*, 7187; M.L. Gee, P.M. McGuiggan, J.N. Israelachvili, and A.M. Homola, *J. Chem. Phys.* **1990**, *93*, 1895; J. van Alsten and S. Granick, *Macromolecules* **1990**, *23*, 4856; S. Granick, *Science* **1991**,*253*, 1374; H. Hu, G.A. Carson and S. Granick, *Phys. Rev. Lett.* **1991**, *66*, 2758; J. Klein and E. Kumacheva, *Science* **1995**, *269*, 816; J. Israelachvili *Intermolecular and Surface Forces*, Academic Press, **1991**.

[14] I. Bitsanis and C. Pan. *J. Chem. Phys.*, **1993**, *99*, 5520.

[15] J. Qian, R. Hentschke, A. Heuer. *J. Chem. Phys.*, **1999**, *111*, 10177.

[16] S. Wong, S. Vasudevan, R.A. Vaia, E.P. Giannelis, D.B. Zax. *J. Am. Chem. Soc.*, **1995**, *117*, 7568. ibid *Solid State Ionics*, **1996**, *86*, 547.